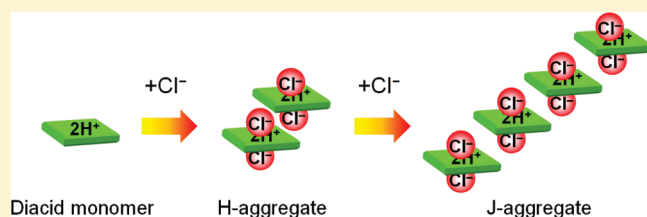


Cl[−] Complexation Induced H- and J-Aggregation of *meso*-Tetrakis-(4-sulfonatophenyl)porphyrin Diacid in Aqueous Solution

Yonbon Arai* and Hiroshi Segawa*

Research Center for Advanced Science and Technology, The University of Tokyo, 4-6-1, Komaba, Meguro-ku, Tokyo, Japan

ABSTRACT: Various porphyrin diacids are known to show controlled self-assembly by inorganic anions. Following the unexpected finding that *meso*-tetrakis(4-sulfonatophenyl)-porphyrin diacid shows Cl[−] specific aggregation in spite of having the anionic substituents, the aggregation behavior of the diacid in aqueous solution with Cl[−] was investigated in detail. We found that Cl[−] induces the H-aggregate, followed by the transformation into the J-aggregate with increasing Cl[−] concentration. For the J-aggregate formation, negatively charged sulfonic acid groups were suggested to be of minor influence. The J-aggregate forms nanoscale macrostructures composed of highly oriented molecules on substrate. To our knowledge, this is the first report of both H- and J-type aggregate formation of a porphyrin diacid in the presence of an aqueous inorganic anion. These results would open the gate for controlling the chromophore packing structure of a porphyrin diacid complexed with an inorganic anion by varying the composition.



INTRODUCTION

Controlling the packing structure of functional dye molecules by supramolecular methods is a challenging task for tailoring functional materials with desired properties.^{1,2} As a result of interchromophoric interactions, perturbations in the electronic absorption spectra of dyes occur. In terms of excitonic coupling, aggregated dyes with blue- and red-shifted absorption bands are referred to as H- and J-aggregates, respectively.³ Due to the distinct optical properties, control of the formation of H- and J-aggregated states of dyes has attracted much research interest.^{4–12}

Porphyrins are important dyes for supramolecular building blocks due to the versatility for structural modifications^{13–15} and the relations to the natural dyes functioning in photosynthetic systems.¹⁶ Recently, supramolecular assemblies of porphyrin diacids have been of growing interests because the aggregate packing structure can be easily tuned through ionic interactions among the cationic core, charged substituents and/or the nature of the inorganic anion.^{17–25} Most intensively studied self-assembly of the diacids is the J-aggregate of *meso*-tetrakis(sulfonatophenyl)porphyrin diacid (H₄TSPP^{2−}) formed in aqueous solution, where the aggregation is facilitated by increasing the concentration of acid or salt.^{17–20} For the J-aggregation, the electrostatic interaction between the anionic sulfonatophenyl groups and the cationic porphyrin core play an important role,²¹ where coexisting inorganic anions are negligibly influential on the packing geometry of the resultant aggregate. On the other hand, Choi et al. demonstrated that tetrakis(4-carboxyphenyl)porphyrin diacid (H₄TCPP²⁺) showed counteranion dependent self-assembly, where J- and H-aggregates of H₄TCPP²⁺ were induced by NO₃[−] and Cl[−], respectively.²² Similarly, nonwater-soluble porphyrin diacids also showed such counteranion induced aggregation phenomenon at the interfaces of organic/water or

air/water.^{23–26} Our group reported that various *meso*-tetraaryl substituted porphyrin diacids formed J-aggregates at the interfaces of aqueous H₂SO₄ solution with CH₂Cl₂ or air.²³ Other groups reported that the interface self-assemblies of tetraarylporphyrin diacids in the presence of aqueous haloacids, HNO₃ and HClO₄ induced J-aggregates, where the position of the absorption peaks depends on the nature of the acids.^{24–26} Under nonaqueous condition, De Luca et al. performed systematic studies on the aggregation behaviors of porphyrin diacids with tetraaryl groups such as sulfophenyl, pyridyl, and hydroxyl in organic solutions using various acids.^{27–29} In these systems, the driving forces of the resultant aggregate structures are relatively explainable in terms of the electrostatic interactions and/or hydrogen bonding among the functional substituent groups, the porphyrin core, and the counteranion. On the other hand, the aggregation of the diacids in the presence of water is less predictable due to weakened ionic interactions and hydrogen bonding in addition to the interactions with water. Empirically, aqueous oxoacid anions such as SO₄^{2−} (HSO₄[−]), NO₃[−], and ClO₄[−] tend to induce J-type aggregates of the diacids, while the role of aqueous haloacid anions on the aggregate type is still unclear.^{22–26}

Recently, Ma et al. performed DFT calculations on the intermolecular interactions of *meso*-tetraphenylporphyrin diacid (H₄TPP²⁺) dimer in the presence of Cl[−] and/or water.³⁰ The calculated results showed that the two most stable diacid dimers consist of slipped parallel arrangements with different slip angles, where the two geometries could induce excitonic interactions

Received: February 24, 2011

Revised: May 12, 2011

Published: May 16, 2011

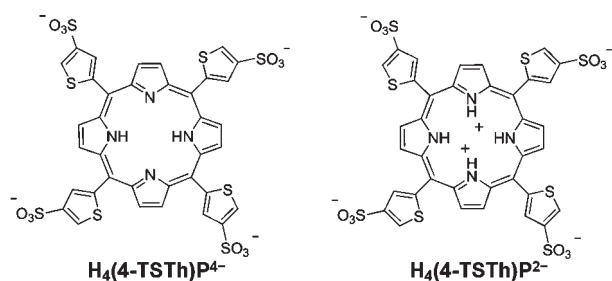


Figure 1. Molecular structures of the free base and the diacid forms of *meso*-tetrakis(4-sulfonatothieryl)porphyrin.

corresponding to H- and J-type aggregates. Since the energetic difference is not significant, this result may explain the observations of both types of aggregates of the porphyrin diacids in the presence of Cl^- .^{22,24,26} Still, the theoretical results are not sufficiently related to the experimental results, where only one type of aggregate was observed.

In our earlier report, we introduced new J-aggregates of water-soluble porphyrin isomers, *meso*-tetrakis(5-sulfonatothieryl)porphyrin diacid ($\text{H}_4\text{T}(5\text{-Sth})\text{P}^{2-}$) and *meso*-tetrakis(4-sulfonatothieryl)porphyrin diacid ($\text{H}_4\text{T}(4\text{-Sth})\text{P}^{2-}$; Figure 1), where the aggregates were efficiently prepared in aqueous solution by increasing the ionic strength.³¹ While the optical properties of the J-aggregates are independent of various oxoacid anions, $\text{H}_4\text{T}(4\text{-Sth})\text{P}^{2-}$ showed Cl^- specific aggregation behavior, which was not observed in the case of $\text{H}_4\text{TSP}^{2-}$ and $\text{H}_4\text{T}(5\text{-Sth})\text{P}^{2-}$. In this study, we performed a more detailed investigation on the aggregation behavior of $\text{H}_4\text{T}(4\text{-Sth})\text{P}^{2-}$ in aqueous solution with Cl^- . Interestingly, we found that $\text{H}_4\text{T}(4\text{-Sth})\text{P}^{2-}$ form both H- and J-type aggregates depending on the concentrations of porphyrin and Cl^- . To this end, the relationship between the Cl^- induced $\text{H}_4\text{T}(4\text{-Sth})\text{P}^{2-}$ aggregates and the reported theoretical results on $\text{H}_4\text{TPP}^{2+}$ dimer with Cl^- ³⁰ is discussed.

EXPERIMENTAL SECTION

$\text{H}_4\text{T}(4\text{-Sth})\text{P}^{2-}$ was prepared by mixing a sufficient amount of protic acid into an aqueous solution of the sodium salt of the free base form ($\text{H}_2\text{T}(4\text{-Sth})\text{P}^{4-}$). The free base salt was prepared by following the procedures in an earlier paper.³² Millipore water was used for all experiments. For pH titration of the monomeric porphyrin, 3×10^{-6} M aqueous solution of the porphyrin with phosphate buffer was used, where pH was adjusted with NaOH and H_2SO_4 . For measurements of the aggregation behavior of the diacid, the sample solutions were prepared by adding equivalent amounts of aqueous solution of protic acids (with salts) into aqueous solution of the free base. After rapid agitation, the solutions were left to rest for ~ 1 h in the dark at room temperature.

Deposited aggregates of $\text{H}_4\text{T}(4\text{-Sth})\text{P}^{2-}$ were prepared by dropping an aliquot of the sample solutions ($10 \mu\text{L}$) on a glass cover. After one minute of immersion, the droplet was blown off quickly. Prior to use, glass covers were cleansed by immersion in $\text{H}_2\text{O}_2/\text{H}_2\text{SO}_4$ (1:3) for 30 min, followed by rinsing in deionized water. To obtain atomic force microscopy (AFM) images, 1 min of aging time and 1 min of immersing time were used.

UV–vis absorption spectra and polarized light absorption spectra were obtained on a Jasco V-570 UV–vis spectrophotometer. For polarized light absorption measurement, a polarizer was set between the sample and the incident light, and the

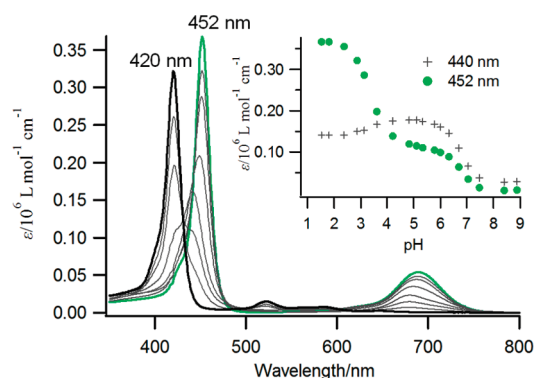


Figure 2. UV–vis spectra of 3.0×10^{-6} M $\text{H}_4\text{T}(4\text{-Sth})\text{P}^{2-}$ in water as a function of pH. Inset shows changes in extinction coefficients at 440 and 452 nm as a function of pH.

incident angle was changed by rotating the sample substrate. Resonance light-scattering (RLS) experiments were performed on a Shimadzu RF-503A spectrofluorophotometer with a 4-mm path length quartz cell by simultaneously scanning the excitation and emission monochromators. Atomic force microscopy images were obtained using Shimadzu SPM-9500 operating in noncontact mode with silicon cantilevers (Nanoworld) with a resonance frequency of ~ 320 kHz. All of the measurements were conducted at ambient conditions.

RESULTS AND DISCUSSION

Protonation of $\text{H}_4\text{T}(4\text{-Sth})\text{P}^{4-}$. Figure 2 shows UV–vis absorption spectral changes of $\text{H}_4\text{T}(4\text{-Sth})\text{P}^{4-}$ in water as a function of pH with the plot of the extinction coefficients at 440 and 452 nm. The plot clearly shows existing of two acid–base equilibria, which gave fitted pK_a values of 6.7 and 3.5. Since the pK_a 's of sulfonic acid groups are normally less than 0,³³ these spectral changes are attributed to the protonation of the two inner nitrogen atoms of the porphyrin ring, where the species with the absorption peaks at around 452 and 689 nm is assigned to the diacid form. The considerably red-shifted absorption and the intensified Q-band of the diacid compared with the free base indicate the increased interaction of the porphyrin ring with the sulfothieryl groups, which can be caused by the structural distortion of the porphyrin ring induced by the diprotonation.³⁴

Aggregation of Monomeric $\text{H}_4\text{T}(4\text{-Sth})\text{P}^{2-}$. Previously, we reported that $\text{H}_4\text{T}(4\text{-Sth})\text{P}^{2-}$ forms J-aggregate with an absorption band (J-band) at around 499 nm in aqueous solution by increasing the concentrations of oxoacids including H_2SO_4 , HNO_3 , and HClO_4 .³¹ While $\text{H}_4\text{T}(4\text{-Sth})\text{P}^{2-}$ shows such coexisting anion-independent aggregation, the J-aggregate was not formed when HCl was used. In order to clarify the role of Cl^- , aggregation behaviors of the diacid in the presence of NaCl and HCl were examined. UV–vis spectra of $\text{H}_4\text{T}(4\text{-Sth})\text{P}^{2-}$ (1×10^{-5} M) in water with 0.1 M HNO_3 and various concentrations of NaCl are shown in Figure 3. The spectra shows that the increase of NaCl concentration causes the decrease of the Soret band absorption of the diacid accompanied with the appearance of blue-shifted bands at around 440 nm. Similar spectral changes were also observed by using comparable concentrations of HCl. Therefore, these results indicate that the blue-shifted species is formed by the complexation of $\text{H}_4\text{T}(4\text{-Sth})\text{P}^{2-}$ and Cl^- , where the cations are not influential on the aggregation. The species was

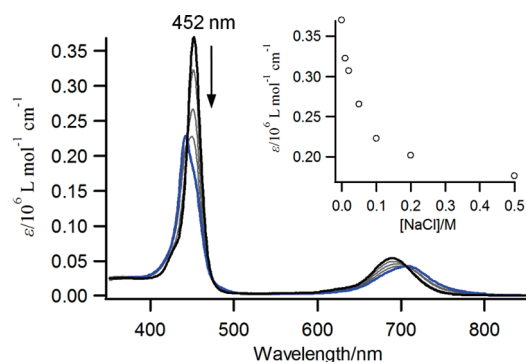


Figure 3. UV-vis spectra of 1.0×10^{-5} M $\text{H}_4\text{T}(4\text{-STh})\text{P}^{2-}$ in water including 0.1 M HNO_3 with various concentrations of NaCl. Inset shows changes in extinction coefficient at 452 nm as a function of NaCl concentration.

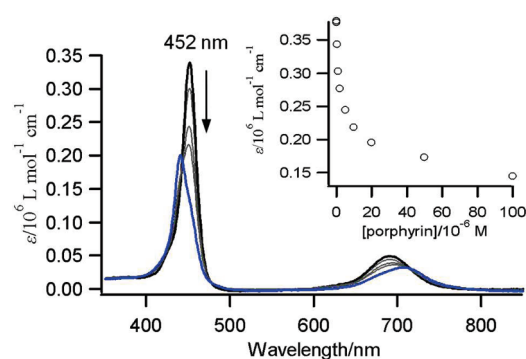


Figure 4. UV-vis spectra of various concentrations of $\text{H}_4\text{T}(4\text{-STh})\text{P}^{2-}$ in water including 0.1 M HCl. Inset shows changes in extinction coefficient at 452 nm as a function of porphyrin concentration.

also effectively formed by the increase of the porphyrin concentration under much higher concentration of HCl than that of porphyrin (Figure 4). The concentration dependence indicates that the origin of the spectral changes can be ascribed to the formation of a stacked porphyrin because the formation of 1:n complex of porphyrin to Cl^- theoretically leads to a constant production ratio of the complex as a function of porphyrin concentration under a sufficiently high HCl concentration. Focusing on the blue-shifted Soret band, this stacked porphyrin will be referred to as H-aggregate.

The H-aggregate solution prepared at a relatively concentrated condition (1×10^{-4} M with 0.5 M HCl) did not show any spectral change after 3 days, which indicates that the H-aggregate does not form extended aggregates. Furthermore, RLS measurements³⁵ were performed for the solutions of monomeric and H-aggregated $\text{H}_4\text{T}(4\text{-STh})\text{P}^{2-}$. Compared with the monomer solution, the H-aggregate solution did not show a distinctly enhanced RLS signal, which supports the small size of the H-aggregate. It should be notable that the spectral changes as shown in Figures 3 and 4 are very similar to those for the dimerization of dueteroporphyrin in aqueous solution,³⁶ where the Soret band decreases in intensity accompanied with the appearance of a new blue-shifted species. Analogously, H-aggregated $\text{H}_4\text{T}(4\text{-STh})\text{P}^{2-}$ is proposed to be the diacid dimer with the similar chromophore packing geometry to the

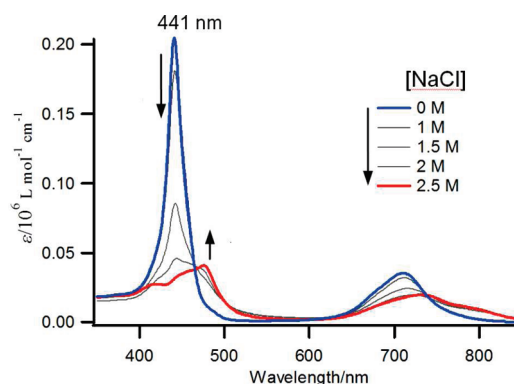


Figure 5. UV-vis spectra of 1.0×10^{-3} M $\text{H}_4\text{T}(4\text{-STh})\text{P}^{2-}$ in water including 0.1 M HCl with various concentrations of NaCl.

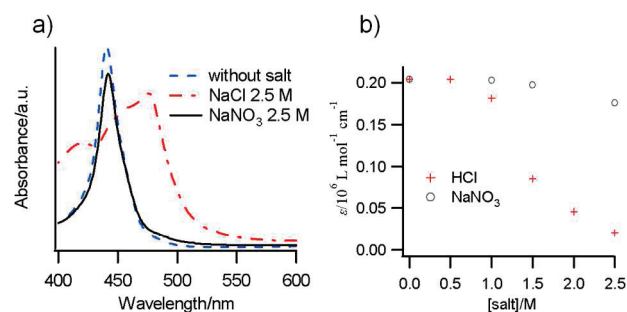


Figure 6. (a) UV-vis spectra of 1×10^{-3} M $\text{H}_4\text{T}(4\text{-STh})\text{P}^{2-}$ in water including 0.1 M HCl, with no salt (broken line), 2.5 M NaNO_3 (solid line), and 2.5 M NaCl (chain line). (b) Changes in extinction coefficients at 441 nm as a function of salt concentrations.

dueteroporphyrin dimer. It is noted that repetitive measurements of the spectral changes during the H-aggregation did not give clear isosbestic points, which may indicate the existence of an intermediate complex.

Structural Transformation of H-Aggregated $\text{H}_4\text{T}(4\text{-STh})\text{P}^{2-}$. Spectral changes of H-aggregated $\text{H}_4\text{T}(4\text{-STh})\text{P}^{2-}$, which was followed by rather quick precipitation, was found to occur with further increasing concentrations of porphyrin and Cl^- . The absorption spectra of $\text{H}_4\text{T}(4\text{-STh})\text{P}^{2-}$ (1×10^{-3} M) with 0.1 M HCl and various concentrations of NaCl are shown in Figure 5. With the increase of NaCl concentration, a new species with the absorption peaks at around 415 and 475 nm was observed to appear with the decrease of the H-aggregate absorbance. Based on the red-shifted band, this type of aggregate will be referred to as J-aggregate. The blue-shifted absorption band can be ascribed to excitonically coupled dipole moments perpendicular to the aggregate axis, where such blue-shifted band is usually accompanied with porphyrin J-aggregation.^{17,22,23,31} The formation of the J-aggregate was not induced by adding NaNO_3 instead of NaCl (Figure 6), whereas HCl caused a similar effect to NaCl (Figure 7a). These results indicate that Cl^- is essential for the transformation of H-aggregate into J-aggregate, whereas the cations are not influential on the transformation. RLS spectra of the aqueous solutions of J-aggregated $\text{H}_4\text{T}(4\text{-STh})\text{P}^{2-}$ showed a significant enhancement of RLS intensity (Figure 7b). This result indicates that the J-aggregate is composed of a large number of porphyrins with electronic interaction. Considering the requirement of

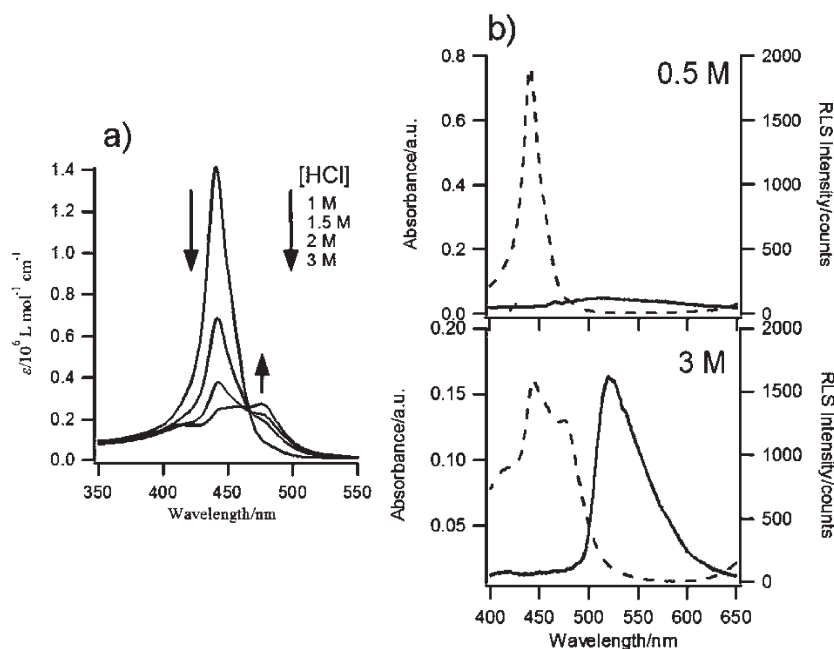


Figure 7. (a) UV-vis spectra of 1×10^{-3} M $\text{H}_4\text{T}(4\text{-STh})\text{P}^{2-}$ in water with various concentrations of HCl. (b) Absorption (broken lines) and RLS (solid lines) spectra of 0.5×10^{-3} M $\text{H}_4\text{T}(4\text{-STh})\text{P}^{2-}$ in water with 0.5 and 3 M HCl.

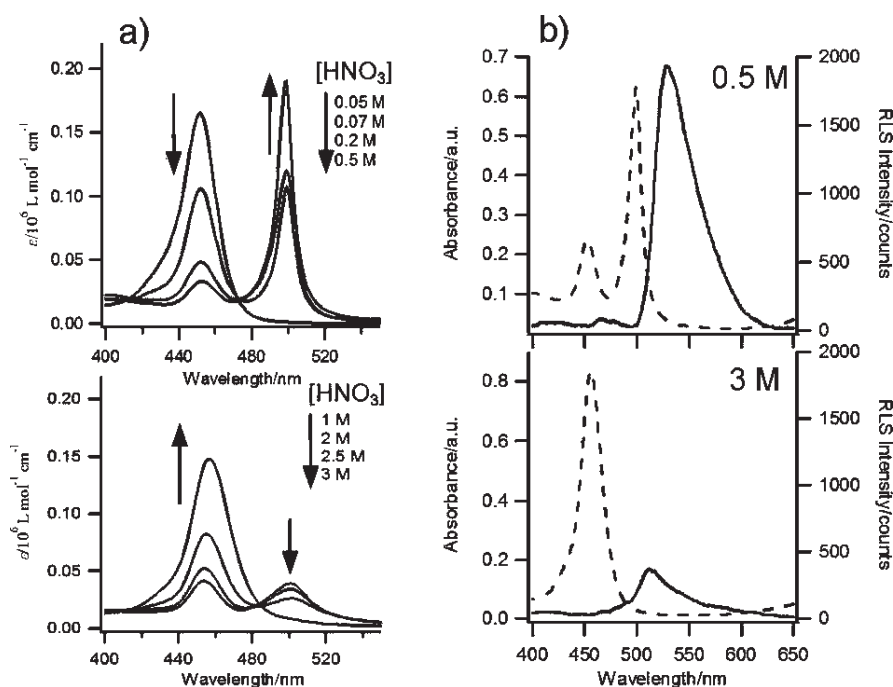


Figure 8. (a) Absorption spectra of 1×10^{-3} M $\text{H}_4\text{T}(4\text{-STh})\text{P}^{2-}$ in water with various concentrations of HNO_3 . (b) Absorption (broken lines) and RLS (solid lines) spectra of 0.5×10^{-3} M $\text{H}_4\text{T}(4\text{-STh})\text{P}^{2-}$ in water with 0.5 and 3 M HNO_3 .

Cl^- for the transformation of H- into J-aggregates, the J-aggregate should be composed of alternating stacks of porphyrin and Cl^- .

It is notable that the spectral feature of the Cl^- induced J-aggregate is clearly different from the coexisting anion-independent J-aggregate,³¹ which emphasizes the important role of Cl^- in the packing of the J-aggregate. Furthermore, we found that the two J-aggregates show different aggregation behaviors in highly acidic concentrations. For coexisting anion-independent

J-aggregate, further increase of HNO_3 concentration caused the decrease of the J-band absorbance with the appearance of an absorption band at slightly longer wavelengths than the monomer band (Figure 8a).³⁷ RLS spectra of $\text{H}_4\text{T}(4\text{-STh})\text{P}^{2-}$ solutions (5×10^{-4} M) with 0.5 and 3 M HNO_3 showed that the disassembly of the J-aggregate caused a significant decrease in RLS intensity (Figure 8b). This result indicates that the increase of acid concentration results in the decrease of the size and/or

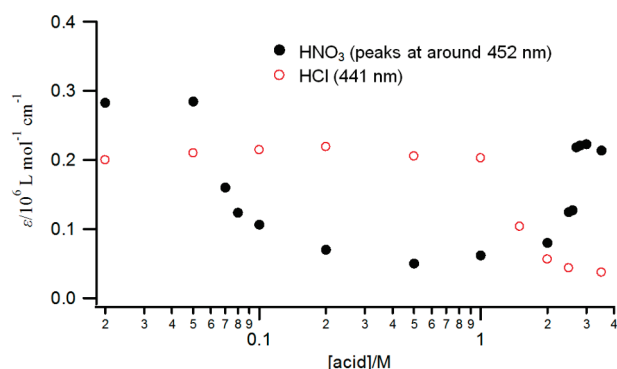


Figure 9. Changes in extinction coefficient of 1×10^{-3} M $\text{H}_4\text{T(4-STh)P}^{2-}$ in water as a function of the concentrations of HNO_3 and HCl . The extinction coefficients of the peak positions at around 452 nm and at 441 nm are plotted for HNO_3 and HCl , respectively.

the number of higher aggregates. It is likely that the highly acidic condition caused the protonation of the negatively charged sulfonic acid groups, resulting in the disassembly of the J-aggregate by the loss of electrostatic and/or hydrogen bond interactions between the diprotonated porphyrin core and the anionic sulfonic acid groups. Notably, a similar phenomenon of the $\text{H}_4\text{TSPP}^{2-}$ J-aggregate was reported by Castriciano et al. using HCl .³⁹ On the other hand, we did not observe a disassembling behavior of the Cl^- induced J-aggregate under similar acidic conditions. In order to clarify the difference, absorbance changes as a function of acid concentration were examined, where the peak absorbances at 441 nm (for HCl) and around 452 nm (for HNO_3) were plotted (Figure 9). The plot shows that the disassembly of the J-aggregate formed with HNO_3 occurs at a concentration of around 2.5 M, where there is no significant absorbance change in the case of the Cl^- induced J-aggregate. Considering that the acid dissociation constant of HCl ($\text{p}K_a = -6.1$) is lower than that of HNO_3 ($\text{p}K_a = -1.4$), these results indicate that the negative charge of the sulfonic acid groups do not play an important role in the Cl^- induced J-aggregation.

Characterization of J-Aggregates Deposited on Substrate. For gaining insight into the aggregate macrostructure, the Cl^- induced J-aggregate was deposited on glass substrates and was characterized by transmission UV–vis spectroscopy and noncontact mode AFM.³⁸

The UV–vis spectral measurements revealed that a substantial decrease in the H-band (blue-shifted band) absorbance occurs in the deposited aggregates compared with that in solution, while the J-band experiences no significant change. To further understand this phenomenon, polarized absorption spectra were taken with s- and p-polarized lights, where the substrate was inclined by 15° with respect to the incident light (Figure 10a). Interestingly, the spectra with the p-polarized light showed a clear H-band at around 410 nm, whereas there was no clear absorption peak around the wavelength in the s-polarized spectra. On the other hand, the J-band showed much stronger absorbance with s-polarized light than with p-polarized one. These results indicate that the transition dipole moments of the H- and J-bands are highly polarized perpendicularly and horizontally to the surface, respectively (Figure 10b). As a result, porphyrin rings in the deposited aggregates are deduced to be highly oriented perpendicularly to the surface. It is noted that such large dichroisms were also observed in the films of other J-aggregates of $\text{H}_4\text{T(5-STh)P}^{2-}$

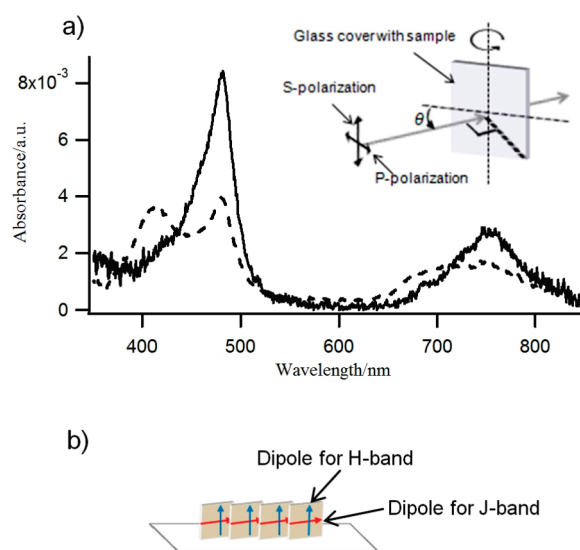


Figure 10. (a) Polarized absorption spectra of the deposited aggregate of $\text{H}_4\text{T(4-STh)P}^{2-}$ prepared from the aqueous solution of 1×10^{-3} M $\text{H}_4\text{T(4-STh)P}^{2-}$ with 2 M HCl on a glass substrate. Inset shows the p-polarized light (broken) and s-polarized light (bold) were taken at the incident angle (θ) of 15° . (b) Presumed arrangement of porphyrin rings in the deposited aggregate, where the J- and H-bands are oriented in parallel and perpendicular directions to the substrate, respectively.

and $\text{H}_4\text{T(4-STh)P}^{2-}$,³¹ whereas we observed much less dichroism in a $\text{H}_4\text{TSPP}^{2-}$ J-aggregate film. With these in mind, it is suggested that the thienyl groups play an important role for the perpendicular orientation. While some alterations in the molecular arrangement in the solid state are presumed, the primary packing structure of the deposited aggregate should be preserved from that in the aqueous environment considering the spectral results.

The AFM observations revealed that the macrostructure of the J-aggregate is rod-shaped on a nanoscopic scale (Figure 11). While most part of the film consists of large agglomerates of the rod-shaped nanostructures (Figure 11a), less agglomerated nanorods with width of 30 ± 10 nm and height of 2.5 ± 0.4 nm were also observed (Figure 11b). Notably, such morphological features are very similar to the nanorods of the J-aggregates of $\text{H}_4\text{TSPP}^{2-}$ and $\text{H}_4\text{T(5-STh)P}^{2-}$.^{31,40–43} Analogous to the possible formation mechanism of the $\text{H}_4\text{TSPP}^{2-}$ nanorod,^{39,41} the $\text{H}_4\text{T(4-STh)P}^{2-}$ nanorod is presumed to be made by the flattening of a nanotube, which is a possible macrostructure in the aqueous suspension state.^{42–44} Taking into consideration the molecular size (~ 1.64 nm),³¹ the height of the nanostructure is rather lower than the sum of the two molecules (~ 3.3 nm). Thus, the nanostructure is presumed to consist of the overlapped molecular layers, where overlapping of the half parts of the molecules gives the height value (~ 2.5 nm) in good agreement with the observed one. It is noted that the observed height of the $\text{H}_4\text{TSPP}^{2-}$ nanorod is comparable to the nonoverlapped bilayer of the molecule.^{40–42} Such difference may originate in their molecular orientations, which were stated on the basis of the results of the polarized absorption measurements. The highly oriented arrangement of $\text{H}_4\text{T(4-STh)P}^{2-}$ in a vertical direction could be favorable for the formation of the overlapped layers, while the presumably less orientated arrangement of $\text{H}_4\text{TSPP}^{2-}$ could hinder the interlayer overlapping.

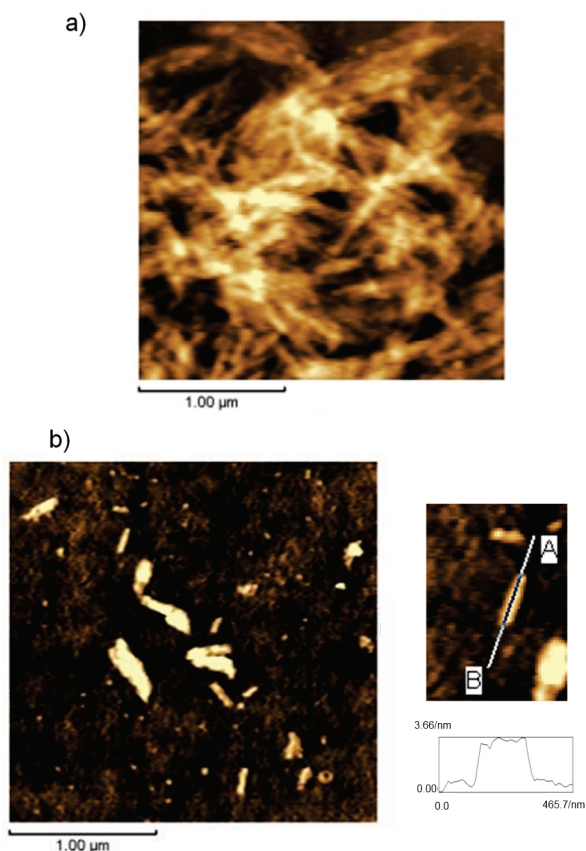


Figure 11. AFM images of the deposited J-aggregate prepared from the aqueous solution of 1×10^{-3} M $\text{H}_4\text{T}(4\text{-STh})\text{P}^{2-}$ with 2 M HCl on a glass substrate: (a) agglomerate of nanorods; (b) less agglomerated nanorods (left) and a magnified image of a nanorod with a height profile at the line AB (right).

Structural Models of H- and J-Aggregates. On the basis of the experimental results, the Cl^- induced H- and J-aggregates were suggested to be the dimer and the one-dimensional array of the diacid, respectively, where the porphyrin rings are bridged by chloride anions. To gain further insight into the stacking structures, the point dipole approximation model in exciton coupling theory³ was adopted to the observed energy shifts of the aggregates. Although this model is a rough estimation, relatively good descriptions were obtained for porphyrin aggregate systems.^{22,47} With consideration of only the nearest neighbor interaction, the point dipole model depicts the energy shift from the monomer absorption (ΔE) as follows:

$$\Delta E = \frac{\mu^2}{2\pi\epsilon_0 r^3} (1 - 3 \cos^2 \theta) \cos \frac{\pi}{N+1} \quad (1)$$

where μ is the transition dipole moment of a dye molecule, r is the distance between the molecule centers and θ is the slip angle. For the H-aggregate, the energy shift ($\Delta E = 550 \text{ cm}^{-1}$) and $N = 2$ under the assumption of $\theta = 90^\circ$ gives $r = 1.43 \text{ nm}$ by eq 1. Considering the size of Cl^- (0.34 nm) and the normal π - π stacking distance of porphyrin (0.35 nm), the calculated intermolecular distance is too larger. Thus, a more realistic geometry would be a modestly slipped stack ($54.7^\circ < \theta < 90^\circ$), where the calculated value of r is smaller than that by $\theta = 90^\circ$. This slipping could be caused by the hydrogen bonding between Cl^- and the two hydrogen atoms on the pyrrolic nitrogens of the

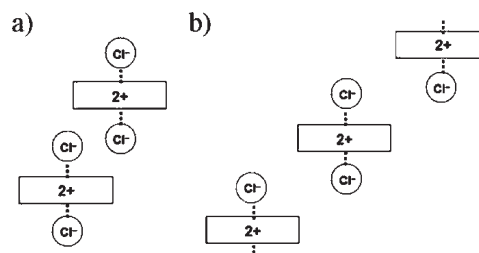


Figure 12. Structural models of the Cl^- induced (a) H- and (b) J-aggregates of $\text{H}_4\text{T}(4\text{-STh})\text{P}^{2-}$. The dashed line stands for hydrogen bond. The size of the porphyrin ring (0.7 nm) and the interplanar distance (0.69 nm) were used for the geometrical relation. In these models, H-aggregate ($54.7^\circ < \theta < 90^\circ$) has some overlap of porphyrin rings, whereas J-aggregate ($\theta = 44^\circ$) has almost no overlap of them.

diprotinated porphyrin, which was observed in crystal structures.⁴⁸ With these in mind, the most possible packing structure of the H-aggregate is a slipped face-to-face dimer bridged by two Cl^- (Figure 12a). For the J-aggregate, the energy shifts of the J-band (ΔE_J) and the H-band (ΔE_H) [$\Delta E_J = -1120 \text{ cm}^{-1}$, $\Delta E_H = 1920 \text{ cm}^{-1}$] under the assumption of $N = \infty$ give $r = 1.17 \text{ nm}$ and $\theta = 44^\circ$ by eq 1. The interplanar distance (0.84 nm) is consistent with the size of stacked porphyrin bridged by Cl^- (0.69 nm). A structural model of the J-aggregate using the calculated values of r and θ with consideration of the hydrogen bonding with Cl^- is shown in Figure 12b. In this edge-to-edge stacking structure, the electrostatic interaction between the cationic porphyrin rings and the chloride anions could not be the main driving force of the structural formation. Thus, other noncovalent interactions are suggested to play a role for stabilizing the J-aggregate structure although specifying them is difficult from our results and qualitative speculations.

Notably, our structural models of $\text{H}_4\text{T}(4\text{-STh})\text{P}^{2-}$ aggregates with Cl^- could be well related to the theoretical stacking structures of $\text{H}_4\text{TPP}^{2+}$ in the presence of Cl^- and/or water on the basis of DFT calculation performed by Ma et al.³⁰ According to the calculation, the two most possible structures are composed of slipped parallel stacked geometries with different slip angles, where Cl^- is hydrogen bonded on the center of porphyrin ring. These structures can correspond to the structural models of Cl^- induced H- and J-aggregates of $\text{H}_4\text{T}(4\text{-STh})\text{P}^{2-}$. For the formation of the structures, Ma et al. concluded that hydrogen bonding between Cl^- and the hydrogen atoms at the 2-position of the phenyl groups play an important role. Analogously, there may exist a strong interaction between Cl^- and the proton at the 3-position of the thienyl groups in the $\text{H}_4\text{T}(4\text{-STh})\text{P}^{2-}$ aggregates. What is more, Ma et al. calculated the binding energies of a one-dimensional infinite array of the diacid and concluded that the stacks with smaller slip angles is more stable than the other one, while the energy of the dimeric forms is the reversed order. This energetics is in good agreement with our observations of the dominant formation of the dimeric H-aggregate at dilute conditions, followed by the transformation into the extended J-aggregates at concentrated conditions. Although the theoretical results are based on the gas molecules, these agreements may indicate that the formations of H- and J-aggregate of tetraaryl substituted porphyrin diacids in the presence of aqueous Cl^- are general phenomena. In fact, various other tetraaryl porphyrin diacids were reported to form H- or J-aggregates with aqueous Cl^- , although either type of aggregate was only observed.^{22,24,26} For

preparing both types of aggregates, the environmental conditions and the influence of the functional groups would need to be considered. In the cases of other sulfonated porphyrin diacids such as $\text{H}_4\text{TSP}^{2-}$ and $\text{H}_4\text{T}(5\text{-STh})\text{P}^{2-}$, we did not observe any Cl^- specific aggregations. Since these diacids form coexisting anion-independent J-aggregates at much more dilute conditions (the equilibrium concentration for half amount of monomer is $\sim 1 \times 10^{-5}$ M with 0.1 M HCl or HNO_3) than $\text{H}_4\text{T}(4\text{-STh})\text{P}^{2-}$ (the equilibrium concentration for half amount of monomer is $\sim 3 \times 10^{-4}$ M with 0.1 M HNO_3), the preferred interactions via their own zwitterionic interactions may have subdued the Cl^- induced aggregations. Taking into consideration even more dilute conditions required for the H-aggregation of $\text{H}_4\text{T}(4\text{-STh})\text{P}^{2-}$ (the equilibrium concentration for half amount of monomer is $\sim 1 \times 10^{-6}$ M with 0.1 M HCl), the Cl^- induced aggregated states of $\text{H}_4\text{TSP}^{2-}$ and $\text{H}_4\text{T}(5\text{-STh})\text{P}^{2-}$ may be less stable than $\text{H}_4\text{T}(4\text{-STh})\text{P}^{2-}$. To better understand the Cl^- induced aggregation of zwitterionic porphyrin diacids, a systematic study using other isomeric porphyrins with mixed 5- and 4-sulfothienyl groups is underway by our group.

CONCLUSIONS

We demonstrated the first observation of both H- and J-type aggregate formation of a porphyrin diacid complexed with an inorganic anion in aqueous solution on the basis of $\text{H}_4\text{T}(4\text{-STh})\text{P}^{2-}$ with Cl^- . The H-aggregate is formed preferably at dilute conditions, followed by the transformation of H- into J-aggregate at more concentrated conditions. For the J-aggregate stacking, the anionic sulfothienyl substituents are of minor influence. When deposited on substrate, the J-aggregate form rod-shaped nanostructures composed of highly oriented molecules. Based on the experimental results and the point dipole model, the stacking structures of the H- and J-aggregates are proposed to be a slipped face-to-face dimer and an edge-to-edge polymer, respectively, where the porphyrins are mediated by two chloride anions. Our results will provide new knowledge for the method to control the stacking structure of porphyrin diacids with inorganic anions.

AUTHOR INFORMATION

Corresponding Author

*E-mail: arai@dsc.rcast.u-tokyo.ac.jp; csegawa@mail.ecc.u-tokyo.ac.jp.

ACKNOWLEDGMENT

We thank Prof. J. Nakazaki, Dr. K. Tamaki, and Dr. J. T. Dy for valuable discussions. This work was supported by Funding Program for World-Leading Innovative R&D on Science and Technology (FIRST) "Development of Organic Photovoltaics toward a Low-Carbon Society" from the Cabinet Office of Japan.

REFERENCES

- (1) Hoeben, F. J. M.; Jonkheijm, P.; Meijer, E. W.; Schenning, A. P. H. *J. Chem. Rev.* **2005**, *105*, 1491.
- (2) Elemans, J. A. A. W.; van Hameren, R.; Nolte, R. J. M.; Rowan, A. E. *Adv. Mater.* **2006**, *18*, 1251.
- (3) Kasha, M. *Radiat. Res.* **1963**, *20*, 55.
- (4) Maiti, N. C.; Mazumdar, S.; Periasamy, N. *J. Phys. Chem. B* **1998**, *102*, 1528.

- (5) Shirakawa, M.; Kawano, S.; Fujita, N.; Sada, K.; Shinkai, S. *J. Org. Chem.* **2003**, *68*, 5037.
- (6) De Luca, G.; Pollicino, G.; Romeo, A.; Scolaro, L. M. *Chem. Mater.* **2006**, *8*, 18.
- (7) Egawa, Y.; Hayashida, R.; Anzai, J. *Langmuir* **2007**, *23*, 13146.
- (8) Yagai, S.; Seki, T.; Karatsu, T.; Kitamura, A.; Wrthner, F. *Angew. Chem., Int. Ed.* **2008**, *47*, 3367.
- (9) Gadde, S.; Batchelor, E. K.; Weiss, J. P.; Ling, Y.; Kaifer, A. E. *J. Am. Chem. Soc.* **2008**, *130*, 17114.
- (10) Ghosh, S.; Li, X.; Stepanenko, V.; Wrthner, F. *Chem.—Eur. J.* **2008**, *14*, 11343.
- (11) Zhao, L.; Ma, R.; Li, J.; Li, Y.; An, Y.; Shi, L. *Biomacromolecules* **2008**, *9*, 2601.
- (12) Delbos, N.; Reynes, M.; Dautel, O. J.; Wantz, G.; Lere-Porte, J.-P.; Moreau, J. J. E. *Chem. Mater.* **2010**, *22*, 5258.
- (13) Drain, C. M.; Alessandro, V.; Radivojevic, I. *Chem. Rev.* **2009**, *109*, 1630.
- (14) Beletskaya, I.; Tyurin, V. S.; Tsivadze, A. Y.; Guillard, R.; Stern, C. *Chem. Rev.* **2009**, *109*, 1659.
- (15) Medforth, C. J.; Wang, Z.; Martin, K. E.; Song, Y.; Jacobsen, J. L.; Shelnutt, J. A. *Chem. Commun.* **2009**, 7261.
- (16) Balaban, T. S. *Acc. Chem. Res.* **2005**, *38*, 612.
- (17) Ohno, O.; Kaizu, Y.; Kobayashi, H. *J. Chem. Phys.* **1993**, *99*, 4128.
- (18) Ribo, J. M.; Crusats, J.; Farrera, J. A.; Valero, M. L. *J. Chem. Soc., Chem. Commun.* **1994**, 681.
- (19) Pasternack, R. F.; Schaefer, K. F.; Hambright, P. *Inorg. Chem.* **1994**, *33*, 2062.
- (20) Akins, D. L.; Zhu, H.-R.; Guo, C. *J. Phys. Chem.* **1994**, *98*, 3612.
- (21) Akins, D. L.; Zhu, H.-R.; Guo, C. *J. Phys. Chem.* **1996**, *100*, 5420.
- (22) Choi, M. Y.; Pollard, J. A.; Webb, M. A.; McHale, J. L. *J. Am. Chem. Soc.* **2003**, *125*, 810.
- (23) Okada, S.; Segawa, H. *J. Am. Chem. Soc.* **2003**, *125*, 2792.
- (24) Zhang, Y.; Chen, P.; Liu, M. *Chem.—Eur. J.* **2008**, *14*, 1793.
- (25) Yamamoto, S.; Watarai, H. *J. Phys. Chem. C* **2008**, *112*, 12417.
- (26) Zhang, Y.; Chen, P.; Ma, Y.; He, S.; Liu, M. *ACS Appl. Mater. Interfaces* **2009**, *1*, 2036.
- (27) De Luca, G.; Romeo, A.; Scolaro, L. M. *J. Phys. Chem. B* **2005**, *109*, 7149.
- (28) De Luca, G.; Romeo, A.; Scolaro, L. M. *J. Phys. Chem. B* **2006**, *110*, 7309.
- (29) De Luca, G.; Romeo, A.; Scolaro, L. M. *J. Phys. Chem. B* **2006**, *110*, 14135.
- (30) Ma, Y. P.; He, S. G.; Ding, X. L.; Wang, Z. C.; Xue, W.; Shi, Q. *Phys. Chem. Chem. Phys.* **2009**, *11*, 2543.
- (31) Arai, Y.; Segawa, H. *Chem. Commun.* **2010**, 46, 4279.
- (32) Arai, Y.; Nakazaki, J.; Segawa, H. *Tetrahedron Lett.* **2008**, *49*, 5810.
- (33) Arnett, E. M.; Ahsan, T.; Amarnath, K. *J. Am. Chem. Soc.* **1991**, *113*, 6858.
- (34) Rosa, A.; Ricciardi, G.; Baerends, E. J.; Romeo, A.; Scolaro, L. M. *J. Phys. Chem. A* **2003**, *107*, 11468.
- (35) Pasternack, R. F.; Collings, P. J. *Science* **1995**, *269*, 935.
- (36) Karns, G. A.; Gallagher, W. A.; Elliot, W. B. *Bioorg. Chem.* **1979**, *8*, 69.
- (37) Figure 6 shows that a considerable decrease in the J-band absorbance occurs at the HNO_3 concentrations between 0.5 and 1.0 M without the increase in the other absorption. This may have originated from the increased inhomogeneous interactions and/or the decrease in the effective absorption cross section due to the increased size of the aggregate.
- (38) For the H-aggregate, we failed to observe well-defined spectra and morphology of the deposited films.
- (39) Castriciano, M. A.; Romeo, A.; Villari, V.; Micali, N.; Scolaro, L. M. *J. Phys. Chem. B* **2003**, *107*, 8765.
- (40) Alexander, D. S.; Deirdre, E. S.; Collin, S. R.; Elizabeth, R. Y.; Walter, F. S.; Julio, C. P. *J. Phys. Chem. B* **2003**, *107*, 11339.

- (41) Rotomskis, R.; Augulis, R.; Snitka, V.; Valiokas, R.; Liedberg, B. *J. Phys. Chem. B* **2004**, *108*, 2833.
- (42) Friesen, B. A.; Nishida, K. R. A.; McHale, J. L.; Mazur, U. *J. Phys. Chem. C* **2009**, *113*, 1709.
- (43) Friesen, B. A.; Rich, C. C.; Mazur, U.; McHale, J. L. *J. Phys. Chem. C* **2010**, *114*, 16357.
- (44) Gandini, S. C. M.; Gelamo, E. L.; Itri, R.; Tabak, M. *Biophys. J.* **2003**, *85*, 1259.
- (45) Kitahama, Y.; Kimura, Y.; Takazawa, K. *Langmuir* **2006**, *22*, 7600.
- (46) Vlaming, S. M.; Augulis, R.; Stuart, M. C. A.; Knoester, J.; van Loosdrecht, P. H. M. *J. Phys. Chem. B* **2009**, *113*, 2273.
- (47) Fuhrhop, J.-H.; Demoulin, C.; Boettcher, C.; Koning, J.; Siggel, U. *J. Am. Chem. Soc.* **1992**, *114*, 4159.
- (48) Stone, A.; Fleischer, E. B. *J. Am. Chem. Soc.* **1968**, *90*, 2735.